Modelling of the adsorption of pharmaceutically active compounds on carbon based nanomaterials

Klaudija Ivanković[1†], Matej Kern[2†] and Marko Rožman[2*]

[1]Faculty of Chemical Engineering and Technology, University of Zagreb, Trg Marka Marulića 19, 10000, Zagreb Croatia

[2] Ruđer Bošković Institute, Bijenička cesta 54, 10000 Zagreb, Croatia

[†]These authors contributed equally to this work

[*]Corresponding author.

Email addresses:

Klaudija Ivanković: kivankovi@fkit.hr

Matej Kern: matej.kern@irb.hr

Marko Rožman: marko.rozman@irb.hr

Abstract

A wide range of pharmaceutically active compounds (PhACs) enter water systems and consequently impact both aquatic and terrestrial ecosystems. Carbon based nanomaterials (CNMs) have emerged as effective next-generation adsorbents, receiving increasing attention due to their potential in water and wastewaters treatment applications. Understanding and acquiring knowledge about the adsorption of PhACs on CNMs is imperative to the chemical engineering applications of CNMs, as well as to risk assessment and pollution control of both CNMs and PhACs. Here we provide a computational assessment of the mechanism and thermodynamics of the adsorption of 18 most common PhACs (acetaminophen, acetylsalicylic acid, atenolol, caffeine, carbamazepine, clofibric acid, diclofenac, fenofibric acid, fluoxetine, gemfibrozil, ibuprofen, ketoprofen, naproxen, phenazone, primidone, propranolol, salicylic acid, tramadol) on four different CNMs (pristine/functionalised graphene and carbon nanotube) in two different solvents (water and *n*-octanol). We show that the adsorption of PhACs on pristine CNMs is controlled by dispersion forces, π interactions and hydrophobic interaction. On the other hand, adsorption on functionalised CNMs is controlled by hydrogen bonding and Coulombic ionic interactions. Furthermore, we demonstrate how functionalization of CNM, CNM curvature and background solution properties modulate the intensity of non-covalent interactions and their contribution towards adsorption Gibbs free energy. With this knowledge, we pinpoint functionalised graphene at environmental pH as the most effective setting for the removal of a given set of PhACs from water and wastewater. Finally, we show that CNMs may transport PhACs into living organisms and release them in nonpolar mediums such as cellular membranes and fat cells. The obtained theoretical insights regarding the adsorption of pharmaceuticals on CNMs expand and complement experimental observations and provide important information that

can contribute to further exploration into the adsorbent properties of CNMs, the evaluation of CNMs toxicity, and towards the development of predictive adsorption models.

Keywords: density functional theory, water and wastewater treatment, environmental fate, solvent polarity, desorption, pH range

1. Introduction

A wide range of pharmaceutically active compounds (PhACs) have been readily detected in wastewaters, freshwater ecosystems and tap water [1]. Although the levels are generally low, due to continuous environmental exposure there is rising concern about potential long-term adverse effects on aquatic ecosystems and consequently on human health [2]. The bioaccumulation of PhACs has been observed at both lower and higher trophic levels in aquatic food webs, e.g. from biofilm to higher predators [3], causing the modification of microbial community composition and hampering natural hormonal functions in fish. Due to food web coupling, PhACs cross ecosystem boundaries and enter terrestrial food webs, thus posing a threat to terrestrial ecosystems. In addition, there is an increasing concern regarding the impact of PhACs on potable water supplies.

Wastewaters of urban, industrial, and agricultural origin have been identified as the main source of PhACs found in waters. Conventional wastewater treatment plants are generally designed to remove pathogens and suspended or flocculated matter and thus only remove a small fraction of PhACs present in wastewater influents [1]. Advanced wastewater treatments like membrane- and nanofiltration, advanced oxidation processes and adsorption have been revealed as promising strategies for the efficient removal of PhACs. In line with the expansion of nanotechnology, wastewater treatment technology has embraced the application of carbon-based nanomaterials (CNMs), such as graphene, nanotubes, fullerenes and their functionalised variants. CNMs have been used in the processes of adsorption [4], photocatalysis [5, 60], electrochemical oxidation [6], nano-membrane filtration [7] and (re)active membranes [8]. It has been suggested that the adsorption of micropollutants on CNMs is one of the most promising treatment methods, encompassing both simplicity and techno-economical attractiveness. Persulfate based advanced oxidation has benefited greatly from the use of an efficient adsorbent [61].. Photocatalysis also benefits from the presence of

an adsorbent where the reaction can take place and CNMs have been used to act as highly efficient adsorbents and enhancers of photocatalytic activity [5]. Similarly, adsorption onto CNMs plays an important role in high-performance electrochemical sensors due to the fact that PhACs are adsorbed prior to electrochemical oxidation on the electrode surface [6]. Active membranes also rely on the adsorption/repulsion properties of CNMs to tailor separation performances [7,9]. Therefore, the exploration of CNMs as more efficient, robust adsorbents for the remediation of wastewater impacted by PhACs has intensified in recent years.

Experimental studies have reported the adsorption of acetaminophen, atenolol, caffeine, carbamazepine, diclofenac and ibuprofen on carbon nanotubes (CNTs) [10–13] as well as the use of graphene or graphene oxide (GO) for the removal of acetylsalicylic acid, acetaminophen, atenolol, caffeine, carbamazepine, diclofenac, ketoprofen and propranolol [9,14–18]. Furthermore, the kinetics and thermodynamics of adsorption have been explored. CNM characteristics such as surface area, curvature, functionalisation and purity have been investigated in relation to the adsorption rate of PhACs [19,20]. The physicochemical properties and characteristics of adsorbate and solution chemistry such as pH, polarity, temperature and ionic strength [15,19,20] were found to play an important role on this adsorption. Each one of these properties may influence these adsorption mechanisms and it is emphasised that further research is still needed to understand the adsorption and develop predictive adsorption models [20]. In order to thoroughly understand and interpret the above-mentioned data, hypotheses were made on the nature of the molecular interactions involved. In addition to hydrophobic interactions, several non-covalent interactions such as hydrogen bonding, ionic, electrostatic and π–interactions have been observed and assumed to play an important role in the adsorption of PhACs on the surface of CNMs [4]. In that context, computational chemistry can reveal the nature and the relative importance of the interactions

involved in sorption and complement the information obtained by experiments. Furthermore, it can predict some of the properties and adsorption affinities of PhACs that have not yet been studied experimentally.

Hitherto, only a handful of theoretical studies on the sorption of microcontaminants on CNMs have been published and of those, the majority were concentrated on tetracycline antibiotics or simple organic model molecules [21–29]. In this work, we computationally evaluated the fundamental properties and behaviour of the 18 most common pharmaceuticals (analgesics, lipid regulators, beta blockers, psychotropic drugs) found in aquatic environments [1,30] during adsorption on CNMs. Single wall CNT, graphene and their functionalised variants, were used as adsorbents. In addition to assessing molecular-level interactions in the sorption mechanism, the effects of curvature and functionalisation of CNMs, as well as the influence of pH, solvent polarity and temperature on adsorption affinity were examined and discussed. By using obtained data, we evaluated the regeneration of studied CNMs and their potential ecotoxicity. We would like to note at this point that antibiotics, as a specific therapeutic class, were not considered in this work and their adsorption on CNMs will be provided in a forthcoming publication.

2. Materials and methods

2.1 Model building.

PhACs: Acetaminophen, acetylsalicylic acid, atenolol, caffeine, carbamazepine, clofibric acid, diclofenac, fenofibric acid, fluoxetine, gemfibrozil, ibuprofen, ketoprofen, naproxen, phenazone, primidone, propranolol, salicylic acid, and tramadol were chosen due to their frequent detection in aquatic environments [1,30]. When available, conformations of the compounds were taken from existing literature; otherwise, geometry optimisations were performed at the B3LYP-D3BJ/6-31g(d) level using the SMD solvation model. The minima on the potential energy surface were confirmed by harmonic frequency analysis. The effect of pH was simulated by the addition or removal of a proton from the model compound on the basis of functional group, pK_a and the pH in question (Table S1 - Supplementary material).

Pristine graphene surfaces that consist of between 54 and 112 carbon atoms were built. Accordingly, zigzag single wall CNTs that consist of between 70 and 110 carbon atoms were built. The edges of CNMs were passivated by hydrogen atoms. In order to attain a reasonable balance of accuracy and computational cost, depending on the size of PhAC, the sizes of CNMs were adjusted. This approach has been successfully used in several studies where the influence of graphene flake size on adsorption energies was much lower than the mean absolute computational error [31]. In addition, C_{60} fullerene was added to help us with the estimation of curvature effect. Although functionalised CNMs are known to contain many kinds of oxygen-bearing functional groups, the models with a low degree of oxidation bearing only hydroxyl and epoxide groups were used [32]. Functionalised graphene used in this study had hydroxyl and epoxide functional groups and it is was referred as graphene oxide while functionalised CNT had only hydroxyl functional groups and it was referred as hydroxylated CNT (HCNT). Fig. S1 (Supplementary material) depicts example geometries of graphene

oxide and HCNT. Simulation of pH was done by the removal of H^+ from the model at pH > 10, at which point the modelled graphene oxide would be dissociated (pK_a = 9) [33]. The same was assumed for CNT. All geometry optimisations were performed using the same approach as for PhACs.

2.2 Adsorption complexes

For each combination of PhACs and CNMs, several interaction configurations were generated. Due to their symmetry, 6 possible spatial orientations were generated for graphene-like structures, while 12 possible spatial orientations were generated for CNTs. In each configuration, the optimised molecule of the pharmaceutical was placed above the optimised surface of the CNMs, approximately in the middle of the CNM structure, to avoid boundary effects. Initial assessment of the complexes was performed with a semi-empirical PM6-D3H4 based method augmented with the empirical correction for the dispersion and hydrogen bonding interactions and the COSMO implicit solvation model. This method showed reasonable accuracy [34] and it was used to establish complexes hierarchy for next-level calculations. From the acquired geometries, the most stable ones, those with no bonding or unrealistic hydrogen transfers, were chosen for subsequent optimisations at the B3LYP-D3BJ/6-31g(d) level of theory. The minima on the potential energy surface were confirmed by harmonic frequency analysis. The employed level of theory was shown to be superior in treating dispersion-dominated supramolecular associations as it represents the best trade-off between accuracy and computational cost [34]. The effect of the solvent was elucidated by the SMD solvation model for water and *n*-octanol [35].

Attempts to identify minima of negatively charged graphene oxide and hydroxylated carbon nanotube PhAC complexes in octanol were unsuccessful due to the problems with SCF

convergence and the default choice of solute cavity, as reported by [36]. The use of extra steps of a quadratically convergent SCF procedure and the use of solvent accessible surface to represent the solute-solvent boundary during geometry optimization followed by single-point energy and frequency calculation that uses the default solute cavity was not feasible at the scale and number of systems examined within this work.

2.3 Computational details.

Adsorption enthalpy (ΔH), which indicates the intensity of interaction between the PhAC and CNM surface, was derived according to the following equation:

$$\Delta H = H_{\text{PhAC-CNM}} - H_{\text{PhAC}} - H_{\text{CNM}} + \text{BSSE}$$

where $H_{\text{PhAC-CNM}}$ is the enthalpy of the adsorption complex, H_{PhAC} is the enthalpy of PhAC, H_{CNM} is the enthalpy of CNM, and BSSE is the basis set superposition error correction. BSSE was calculated to eliminate the effect for basis set incompleteness by employing a counterpoise correction method [37]. The use of counterpoise correction was also found to result in a greater decrease in mean unsigned error than the transition from a double zeta to a triple zeta basis set [58]. Vibrational frequencies were obtained by harmonic frequency analysis and, as previous work found the scaling factor is very close to one [59], were not scaled. Using the same adjusted equation, adsorption Gibbs free energy (ΔG) was calculated. Final ΔG was corrected for the ΔG change associated with moving from a gas-phase pressure of 1 atm to a liquid-phase concentration of 1 M. Atomic charges were obtained by the use of the cm5 model as implemented in multiwfn 3.7 [38]. Enthalpies of hydrogen bond formation ($\Delta H_{\text{H-bond}}$) were calculated from the redshift of donor – hydrogen stretching vibration (Δv in

194 cm^{-1}) using Iogansen's relationship and summed for all existing hydrogen bonds in a
195 complex, ($\Delta H_{\text{H-bonds}}$) [39]:

$$\Delta H_{H-bond} = \sqrt{1.92(\Delta\nu - 40)}$$

$$\Delta H_{H-bonds} = \sum \Delta H_{H-bond}$$

196 All semi-empirical calculations were performed using Mopac2016 software (MOPAC2016,
197 James J. P. Stewart, Stewart Computational Chemistry, Colorado Springs, CO, USA), while
198 DFT calculations were performed using Gaussian 16 [40].
199
200

3. Results and Discussion

3.1 Thermodynamic parameters and performance against the experimental data

The computed E_{ads} and thermodynamic parameters in water and octanol are listed in Table S2 - Supplementary material (due to large amount of data provided). The range of the E_{ads} and ΔH values suggests an exothermic nature of the adsorption. All the ΔS values are negative, indicating that adsorption is associated with ordering. Negative ΔH and ΔS values indicate that the spontaneity of the reaction (ΔG) is temperature-dependent. ΔG values at 298K are generally negative, suggesting that the studied PhACs are spontaneously adsorbed on the studied CNMs. Prior to a general discussion, a few words on the performance of our model against the experimental data.

A comparison of the ΔG values obtained by the employed theoretical model with available experimental data show that calculated ΔG values are systematically lower than the experimental ones. The mean unsigned error is 19.96 kJ mol^{-1}, which is slightly better than the performance of the SMD model in the solvation free energies at the B3LYP/6-31G(d) level of theory for ions in water that exhibited a mean unsigned error of 20.48 kJ mol^{-1} [35]. Except for the computational error of the model, any difference between experimental and theoretical values may be attributed to differences between the model and real-life system. Our model CNMs are of uniform size and have a homogeneous surface and strictly defined functional groups (for functionalized CNMs). On the other hand, real life CNMs can have defective surfaces with vacancies, wrinkles and folds, form bundles with grooves and intestinal channels and non-uniform and imperfect functionalization [19,20]. Furthermore, this study does not consider ionic strength of the solution as well as competitive adsorption. However, a good agreement with the reference experimental data, found in table S3, indicates

that the employed model can reproduce the chemical phenomena behind the adsorption of studied the PhACs on CNMs sufficiently well.

3.2 Adsorption mechanism

The obtained ΔH values are generally > -60 kJ mol^{-1} and there is no apparent chemical bond formation (Table. S2), thus categorising the observed adsorption interactions into physisorption, in agreement with general observations on the adsorption of organic molecules onto CNMs. Physisorption is caused by the non-covalent interactions between adsorbates and adsorbents. Electrostatic, hydrogen bonds, Van der Waals (vdW) and π interactions usually act together with changing relative contributions, causing the adsorption of PhACs on CNMs. The relative contributions of certain categories of non-covalent interactions are modulated by the properties of the PhACs, CNMs and the solution. Several recent reviews have emphasised the need to systematically understand the nature of the molecular interactions associated with the adsorption of PhACs on CNMs in order to interpret the obtained experimental data [19,20]. Along these lines, we examined the relationship between certain categories of non-covalent interactions and adsorption energy.

3.2.1 van der Waals dispersion forces

Dispersion interaction was pinpointed as one of the main interactions governing the adsorption of molecules on CNMs [41,42]. Since vdW dispersion energy is proportional to the polarizabilities of the interacting entities, average molecular polarisability has been used to describe the intensity of vdW interactions during adsorption [41]. Average molecular polarisability was used here to display the change in contribution of vdW dispersion interactions to the energy of adsorption. Strong Spearman correlations between vdW and adsorption enthalpy were found for graphene (r_s = -0.68, p < .05), CNT (r_s = -0.59, p < .05) and fullerene (r_s = -0.43, p < .05), suggesting a meaningful contribution of vdW dispersion interactions to the adsorption ΔH for pristine CNMs (Fig. S2 – Supplementary material). A

252 decrease in the contribution of induce dipole-induce dipole interactions in the order of
253 fullerene<nanotube<graphene was observed. The observed trend is the consequence of the
254 size of the CNM molecule. Larger molecules have more electrons and with more electrons,
255 the outer electrons are more easily displaced, which gives a larger molecule a higher ability
256 for stronger induced dipole interactions. The size of the contact surface also contributes to the
257 observed trend, because the contact surface of the CNM through which the CNM interacts
258 with PhACs decreases in the following order: fullerene<nanotube<graphene. Analysis of the
259 correlation by charge of molecular entity shows the strongest correlation for anions ($r_{s(graphene)}$
260 = -0.85, $p < .05$), followed by neutrals ($r_{s(graphene)} = -0.7$, $p < .05$) and lack of correlations for
261 cations ($r_{s(graphene)} = -0.66$, $p > .05$), Fig. S3 – Supplementary material. This is to be expected,
262 as negative ions with excess electrons are more easily polarized compared to the denser
263 electron clouds of cations. It should be noted that the correlation between the molecular
264 polarisability of cations and the ΔH of the adsorption for graphene and nanotube is not even
265 statistically supported. This latter observation is consistent with the lack of correlation
266 between adsorption energies and dispersion when strong electron acceptor-substituted
267 benzene rings interact with graphene moiety [42]. It has been suggested that the strong charge
268 transfer absorbed into the induction energy caused the lack of correlation between interaction
269 and dispersion energies.

270 The presence of OH groups on the surface of CNMs has a large effect on the contribution of
271 vdW dispersion interactions. A statistically supported correlation between vdW interactions
272 and ΔH of the adsorption was only detected for graphene oxide ($r_s = -0.54$, $p < .05$), Fig. S2 –
273 Supplementary material. This is expected due to the introduction of additional interactions
274 such as hydrogen bonds. The formation of hydrogen bonds negatively affected vdW forces in
275 two ways. Firstly, the average distance between CNMs and PhACs increased by 0.7 Å due to
276 the formation of hydrogen bonds, causing Van der Waals attraction forces to exponentially

drop. Secondly, functionalization introduced sp^3 carbons onto the surface of CNMs, which had the overall effect of lowering the isotropic polarizability of the graphene oxide flake, in comparison with the pristine graphene flake, particularly for larger flake sizes.. The fact that a meaningful contribution of vdW dispersion interactions to adsorption ΔH was detected for graphene oxide should be attributed to the effects of size of the CNM molecule.

Change of solvent polarity towards a lower dielectric constant (*n*-octanol) did not affect the contribution of vdW interactions towards ΔH of the adsorption, Fig. S2 – Supplementary material. Although the polarisability of molecules decreased in the lower dielectric medium and the lower permittivity of *n*-octanol led to an increase of the contribution of electrostatic interactions, the correlation of the polarizability of the PhACs molecules and adsorption energy remained high for neutral and negatively charged molecules on both pristine graphene and CNT, Fig. S3 – Supplementary material. This altogether indicates that, in an environment that enhances electrostatic interactions, vdW dispersion interactions remain an important contributor to the stabilisation of the adsorption complex.

3.2.2 π interactions

π interactions were suggested to play a prominent role in the process of the adsorption of PhACs onto CNMs [4]. Two types of π interactions played the most prominent role in the formation of the PhACs–CNM associates: I) The π–π interaction, a type of dispersion force established between two unsaturated (poly)cyclic systems and II) the ion−π interaction, essentially the electrostatic interaction between ion and negatively charged electron cloud of π systems. Tang et al. (2020) used LOLIPOP (Localized orbital locator-integrated π over plane) index values to explain the role of π interactions in the adsorption of aromatic compounds on graphene oxide and found a partial relationship between LOLIPOP indices and the interaction

ability of adsorbent and adsorbate [21][21](Tang et al. 2020)(Tang et al. 2020). We, however, found no correlation between LOLIPOP index values and the Δ*H* adsorption values (Fig. S4 - Supplementary material). The reason for this may lie in the increasing complexity of adsorbent molecules, PhACs used in our case versus simple aromatic compounds used by Tang et al. [21].

In order to assess the contribution of π interactions to adsorption processes, we examined the difference in Δ*H* adsorption between a set of PhACs with one aromatic ring against a set of PhACs with two aromatic rings (separated or fused). Both sets contained 9 molecules. Molecules from both sets were adsorbed onto CNMs though the parallel-displaced configuration interacting preferably via π–π stacking, Fig. S5 a) - Supplementary material. Statistically significant differences between compounds with one ring and compounds with two rings were found for both graphene and CNTs ($t(16) = 2.69$, $p<.05$; $t(16) = 2.93$, $p<.05$, respectively (Table S4 – Supplementary Material)). On average, the additional π system resulted in a 14.7 kJ mol^{-1} lower Δ*H* of the adsorption for graphene and 10.4 kJ mol^{-1} for CNTs, suggesting a strong role of the additional π system in stabilising the PhACs – CNM complex. This observation highlights the important contribution of π–π interactions to the adsorption energy. On the other hand, functionalised CNMs do not exhibit statistically significant differences in adsorption Δ*H* between compounds with one ring and compounds with two rings, suggesting reduced role of the additional π system (Table S4 – Supplementary Material). The presence of sp^3 carbons on the functionalised CNM surface alters the conjugated structure and reduces π–electron-donating ability, therefore lessening the possibility of π-stacking interactions, Fig. S5 b) - Supplementary material. Similar results were seen in He et al. (2018), who reported weakened π–π interactions between graphene oxide and tetracycline as a result of the decreased π–electron-donating ability of the graphene oxide surface. It is important to note that effect of reduced role of the additional π system due

to functionalization is stronger for functionalised CNT and that at $p<.06$ graphene oxide exhibit significant differences in adsorption ΔH between compounds with one ring and compounds with two rings (Table S4 – Supplementary Material), suggesting a relevant contribution of π–π interactions to the adsorption ΔH of graphene oxide due to larger surface plane. Along these lines, graphene and/or CNT oxide with a relative low number of OH groups and large sp^2 regions (the opposite of those used here) may have a strong contribution of π interaction energy towards ΔH of the adsorption. On average, graphene showed a larger difference between one and two rings sets than CNT, which can be correlated to the larger planar surface area of the π system available for stacking interaction.

Introduction of the charge to PhACs influences the nature of π interactions by introducing an additional ion-π interaction. Positive PhAC-pristine CNM complexes are on average 8.2 kJ mol^{-1} more stable than neutral PhAC-pristine CNM complexes. Difference may be attributed to interactions of the positively charged cation moiety with the negatively charged electron cloud of π systems. The anion–π interaction displays the opposite trend and leads to a complex destabilisation by an average of 10.3 kJ mol^{-1}. Depending on the conformation of the complex observed, the ion-π interaction is either strong or mild. If the charge is close to the π of the systems as it is in e.g. acetylsalicylic acid or atenolol (Fig. 1 a) and c)), the ion-π interaction displays a strong effect on complex stabilisation. Protonated atenolol-graphene complex is 10.7 kJ mol^{-1} more stable, while deprotonated acetylsalicylic acid is 18.2 kJ mol^{-1} less stable than its neutral form. On the other hand, a mild ion– π interaction takes place when the ion is further away from the negatively charged electron cloud of π systems as it is in e.g tramadol cation or clofibric acid anion (Fig. 1 b) and d)). Protonated tramadol-graphene complex is 3.4 kJ mol^{-1} more stable, while deprotonated clofibric acid is 5.1 kJ mol^{-1} less stable than its neutral form. Atenolol and acetylsalicylic acid complexes show a 5 to 7 times

greater charge transfer upon ionisation than tramadol/clofibric acid complexes, further confirming a strong interaction.

In addition, charged functional groups may act as electron withdrawing/donating substituents, which further enhance/reduce the π-stacking interaction. As an illustrative example, the negatively charged carboxylic group of acetylsalicylic acid increases the electron density in the π-cloud of the substituted ring, which increases the electrostatic repulsion with the π-system of the nanomaterial, reducing the π-stacking interaction, (Fig. S6 - Supplementary material). On the other hand, the highly basic group of carbamazepine (pK_a 13.9) upon protonation increases cumulative charge of the closest six-membered ring by +0.065 e, leading to an observed increase in complex stability, even though the charged group is not close to the graphene surface. A similar mutual influence of cation– π and π – π interactions was detected for benzene model systems [43].

A significant difference in adsorption Δ*H* between neutral compounds with one and two rings was also observed for both graphene and CNT complexes dissolved in *n*-octanol (13.7 and 11.03 kJ mol^{-1}, respectively (Table S4 – Supplementary material)). The latter further supports our previous observation regarding the important contribution of π–π interactions to the adsorption energy. It is important to note that the adsorption Δ*H* of the complexes in n-octanol is lower than in water. However, the difference is mainly due to solvatation/desolvatation effects which is consistent with observations on the inverse correlation of complexation constant with solubility of fullerene in various solvents [44].

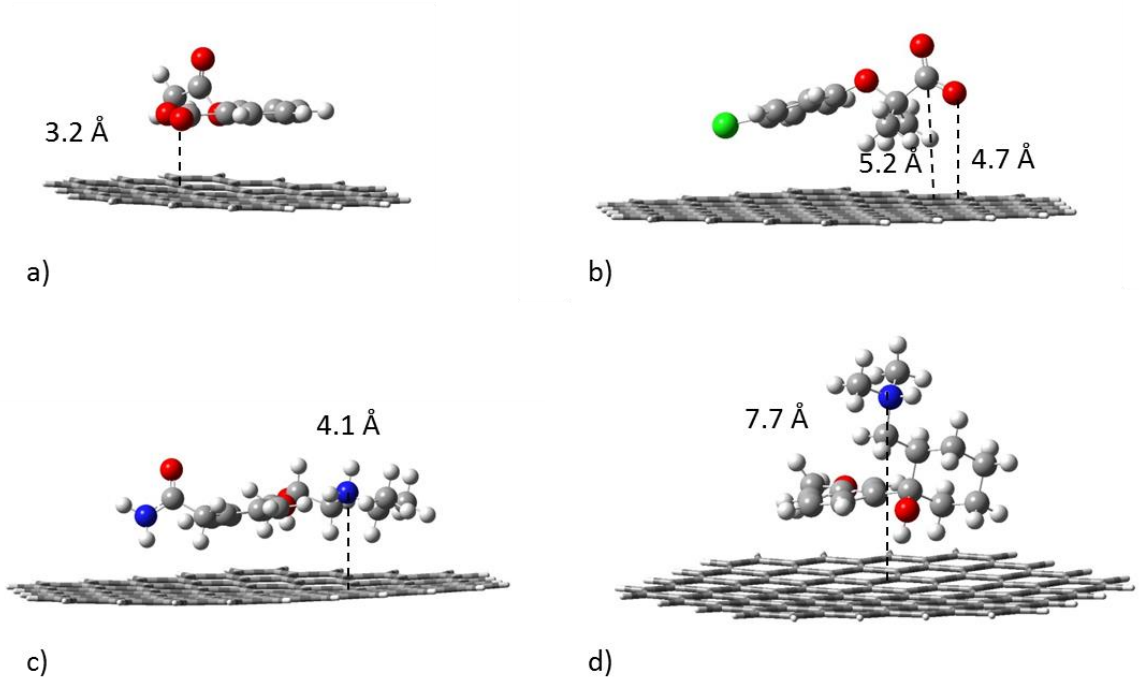

371

372 Fig. 1: B3LYP-D3BJ/6-31g(d) optimized complex of pristine graphene with: a) deprotonated
373 acetylsalicylic acid, b) deprotonated clofibric acid, c) protonated atenolol and d) protonated
374 tramadol.

375

376 ## 3.2.3 Hydrogen bonding

377 The functionalization of CNMs, among other things, enables the formation of hydrogen bonds
378 between CNMs and PhAC molecules, and hydrogen bonding has been suggested as one of the
379 mechanisms that contribute to adsorption [20]. The functionalization of CNMs resulted in
380 enthalpic gains, especially for cationic and anionic complexes, Fig. 2 b). Enthalpic gains
381 changed the complex stability ladder from cation>neutral>anion for pristine CNMs to
382 cation>neutral≈anion for functionalised CNMs, Fig. 2 b). Obtained enthalpy gains of
383 functionalised CNTs (compared to functionalised graphene) imply a significant role of
384 hydrogen bonds. Authors have been assessing the strength of hydrogen bonds on the basis of
385 bond length and angle between functional groups [21,28]. Although this approach

demonstrated its functionality, it is constrained by both nominal values and number of comparisons. Due to the volume of data, we estimated the enthalpy of formation of an hydrogen bond through the change of the proton-stretching vibration [39]. First we found an strong correlation (functionalized graphene r_s= -1, p < .05, functionalised CNT r_s = -0.8, p < .05) between the mean number of hydrogen bonds and the mean adsorption ΔH, suggesting that complexes with a larger number of hydrogen bonds are more stable, Fig. S7 – Supplementary material. The total hydrogen bonds ΔH ($\Delta H_{\text{H-bonds}}$) of a given PhAC-CNM complex correlates well with the change in adsorption ΔH from pristine to functionalised CNMs. Correlation is strong for CNTs (r_s= -0.79, p < .05) and moderate for graphene (r_s = -0.51, p < .05), indicating a considerable contribution of hydrogen bonds to the observed differences in adsorption ΔH between functionalised and pristine CNMs, (Fig. S8 Supplementary material). These results relate to recent findings about the significant roles of hydrogen bonds in tetracycline-graphene oxide complexes [25]. Moderate correlation between the total hydrogen bonds ΔH and the adsorption ΔH (r_s = -0.42, p < .05) was detected only for oxidized CNTs (Table S5 - Supplementary material). The lack of correlation for functionalised graphene may be attributed to the balance between the contribution of hydrogen bonds and other non-covalent interactions. As it was shown, functionalized graphene has a statistically supported contribution of dispersion, while functionalized CNT does not. Also, there is indication for relevant contribution of π–π interactions to the functionalized graphene adsorption ΔH. Here we hypothesized that dispersion, π interactions and hydrogen bonds contribute to the stabilization of adsorption complexes for both functionalised CNMs. However, the contribution of dispersion and π interactions is higher for functionalized graphene, while functionalized CNTs have a higher contribution of hydrogen bonds energy. With this in line, the higher enthalpic gains of functionalised CNT compared to functionalised graphene can be rationalised by the prevailing hydrogen bonds energy term.

The strongest hydrogen bonds were observed in anionic molecular entities, followed by neutral complexes and cations (Table 1), a finding consistent with prior research that has shown the larger hydrogen bonding basicity of carboxylates in comparison with carboxylic acids and the change in behaviour of secondary amines upon proton capture from hydrogen bond acceptors to hydrogen bond donors [45,46]. The average number of hydrogen bonds that molecules form also varies depending on their ionic form. Graphene oxide forms 3 hydrogen bonds per molecule while hydroxylated CNTs 1.9 – a consequence of the availability of hydroxyl groups due to curvature effect. Cationic and anionic complexes mainly form more hydrogen bonds than neutral complexes, Table 1. This stems from the change in both type and number of hydrogen bonds accompanying the (de)protonation of PhAC functional groups. The total hydrogen bonds enthalpy increases in the order of anionic<cationic<neutral complexes, indicating the largest impact of hydrogen bonds on the stability of anionic complexes, Table 1. This explains why the adsorption ΔH ladder changes from cation<neutral<anion for pristine CNMs to cation<anion≈neutral for functionalised CNMs.

In octanol, all observed trends regarding hydrogen bonds remained as they were in water, Table 1. Moreover, the total hydrogen bonds enthalpy did not change significantly between water and *n*-octanol, indicating that the strength of hydrogen bonds within complexes does not change with a decreasing dielectric constant of solvent. These findings are in contrast with previous findings on small model systems that suggest stronger hydrogen bonds with a decreasing dielectric constant of solvent [47]. On the other hand, the small model systems considered in the study were full hydrated in contrast to our complexes, where some hydrogen bonds were formed outside the water-accessible surface area (Fig.3), which we believe reduced the negative impact of water on hydrogen bonds.

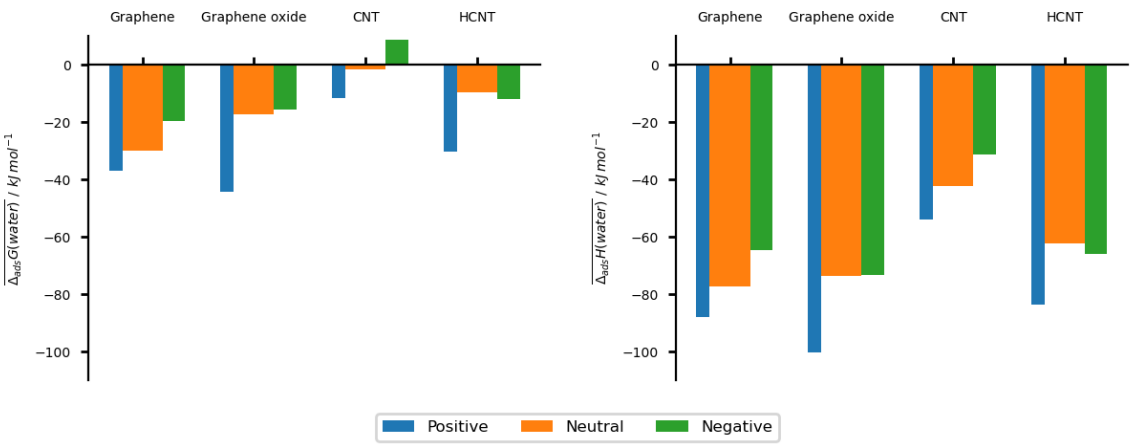

435

436 Fig. 2. Mean adsorption Gibbs free energy and enthalpy of CNM complexes broken down by

437 charge of a complex.

438 Table 1. hydrogen bond properties of functionalised CNM complexes by charge and solvent.

Solvent	CNM	Charge	Mean $\Delta H_{\text{H-bonds}}$ (kJ mol^{-1})	Mean number of hydrogen bonds	Pooled mean hydrogen bond ΔH(kJ mol^{-1})
water	Graphene oxide	+	-55.04	3.83	-14.37
		neutral	-41.31	2.24	-19.52
		-	-63.96	3.00	-22.16
	HCNT	+	-32.25	2.40	-16.54
		neutral	-24.13	1.69	-14.18
		-	-37.20	1.56	-25.82
n-octanol	Graphene oxide	+	-51.48	3.83	-13.93
		neutral	-34.08	2.33	-15.42
		-	-69.43	3.11	-23.21
	HCNT	+	-30.73	1.67	-22.35
		neutral	-25.56	1.60	-17.05
		-	-45.95	1.89	-25.44

439

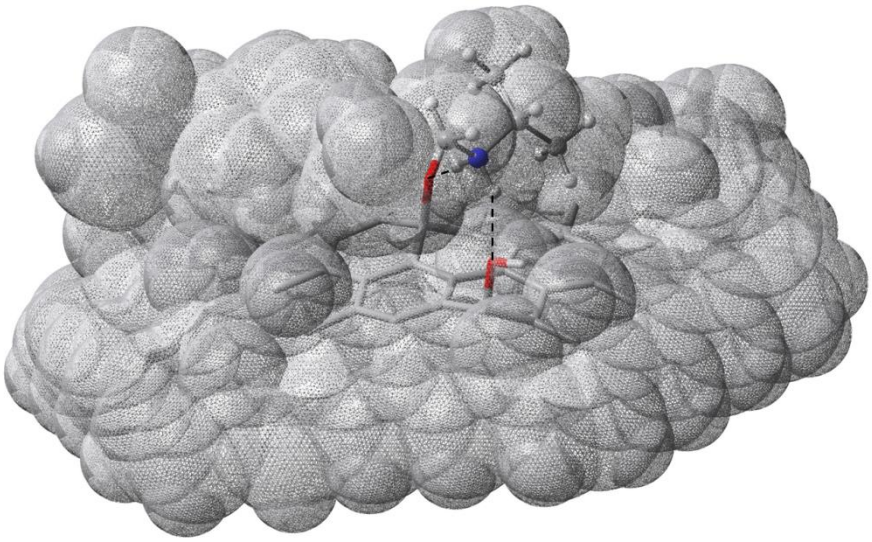

Fig. 3. B3LYP-D3BJ/6-31g(d) optimized geometry of the positive atenolol-graphene oxide complex. Spheres are showing complex solvation cavity. Protonated amine hydrogen bonds are placed outside the water-accessible area Due to clarity of representation majority of the complex structure is omitted.

3.2.4 Coulombic ionic interactions

The pKa of graphene oxide and hydroxylated CNTs is around 9 [33] and it is expected that at pH levels above 10, OH groups on CNM surfaces become negatively charged, putting forward ionic electrostatic interactions as the dominant mechanism in controlling the adsorption of PhACs on negatively charged graphene oxide or hydroxylated CNTs. Since Coulombic interactions are very strong interactions, the adsorption complex between positively charged PhACs and negatively charged CNMs is extremely stable, as can be observed in the case of carbamazepine. Intuitively, it is opposite in the case of the interaction between negatively charged PhACs and negatively charged CNMs. The calculated positive ΔG values for all “negative-negative” adsorption complexes indicated no spontaneous

457 reaction. The rapid decrease of adsorption capacity due to the negative surface charge of the
458 functionalised CNMs and the deprotonated functional groups of PhACs is also reported in
459 experimental data (Guerra et al. 2019; Tang et al. 2020). Complexes with hydroxylated CNTs
460 exhibit a positive ΔH, suggesting an endothermic process. In contrast to this, the adsorption of
461 negatively charged PhACs on negatively charged graphene oxide is mainly exothermic.
462 Although initially surprising, this result is rationalised by carefully examining the structure of
463 the complexes in place. Conformations are maximising the distance between negatively
464 charged groups thus minimising Coulombic repulsion and if available form hydrogen bonds
465 and interact via T-shaped configuration. It is suggested that the T-shaped configurations enjoy
466 a favourable interaction of the positive quadrupole of the benzene ring and the negative
467 quadrupole of the sp^2 region, as seen on benzene dimer systems [49]. For example
468 deprotonated acetaminophen complex with deprotonated graphene oxide minimise Coulombic
469 repulsion, forms the hydrogen bond and forms T-shaped configuration. In a T-shaped
470 configuration the acetaminophen substituted benzene ring have a potential to interact with
471 small undistorted sp^2 region on the graphene surface.

472

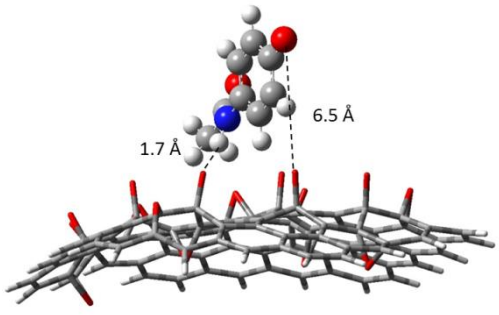

473

474 Fig. 4. Deprotonated acetaminophen complex with deprotonated graphene oxide at the
475 B3LYP-D3BJ/6-31g(d) level of theory.

476

3.2.5 Hydrophobic interactions

Neutral pharmaceuticals show a lower complexation ΔG in water compared to *n*-octanol. Graphene and CNT complexes are, on average, 14.9 and 11.3 kJ mol^{-1}, respectively, more stable in water than in *n*-octanol. This result is consistent with observations on molecular tweezers-fullerene associations, where increases were reported following decreasing solubility of the fullerene [44,50]. The fact that this interaction is stronger in polar solvents due to the less solvated nonpolar surfaces demonstrates that the complexation interaction is hydrophobic in nature [51]. The obtained negative enthalpies and entropies of complexation (Table S2 – Supplementary material) suggest that complexation is enthalpy-driven, indicating a nonclassical (enthalpic) hydrophobic effect [51]. Moderate correlation ($r_{s(graphene)}$ = -0.60, p < .05, $r_{s(CNT)}$ = -0.58, p < .05) between complexation ΔG and differences in the solvent-accessible surface area of the interacting particles before and after the association additionally confirms the nonclassical hydrophobic effect [51], Fig. S9. Supplementary material. Desolvation of the fullerene, dispersive interactions within the complex and solute–solute dispersion interactions were listed as dominant factors governing the hydrophobicity of fullerene [44,50,51].

3.3 The effect of CNM properties on adsorption of PhACs

3.3.1 CNM curvature effect

Our calculations show a strong positive correlation between CNM curvature and ΔG of adsorption, Fig.5. Similarly, previous studies observed that significant differences between the adsorption amounts of simple aromatics on CNTs were caused by CNT curvature [26,27,52]. Expressing curvature as the amount by which CNM surface deviates from being a

plane confirms that the adsorption of PhACs becomes more exotermic in the order of fullerene<nanotube<graphene. As already noted through our discussion, both vdW dispersion and π interactions are related to contact surface and, consequently, PhACs maximise their interaction if CNM is less curved. In addition, PhACs form more hydrogen bonds with less curved functionalised CNMs, leading to overall stronger adsorption interactions.

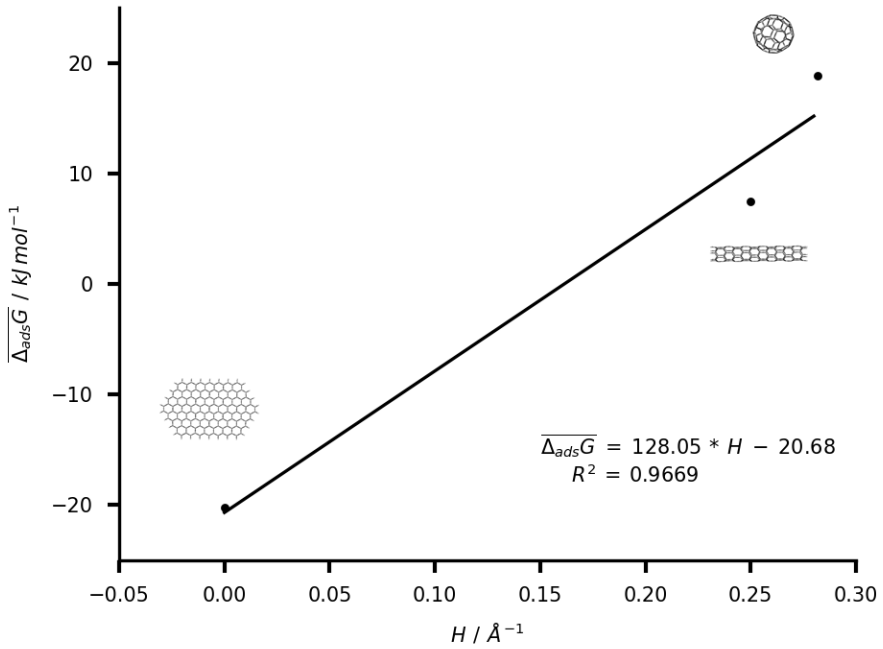

Fig 5: Regression of CNM surface curvature and mean Δ*G* of adsorption.

3.3.2 Functionalization of CNM

Previous discussion suggests that the functionalization of CNMs via introduction of hydroxyl and carbonyl groups strongly affects all non-covalent interactions between PhACs and CNMs. While it reduces vdW and π interactions, it enables the formation of hydrogen bonds and (at certain pH levels) Coulombic ionic interactions. In addition, the introduction of OH groups decreases CNM surface hydrophobicity [4,20], thus reducing the hydrophobic effect in the

polar solvent. Altogether, the functionalization of CNMs resulted in high enthalpic gain for cationic and anionic complexes due to the formation of strong hydrogen bonds changing the complex stability ladder from cation>neutral>anion for pristine CNMs to cation>neutral≈anion for functionalised CNMs, Fig. 2. b). On the other hand, enthalpic gains due to functionalisation are partly cancelled out by higher entropic losses (~10 kJ mol^{-1} larger for functionalised CNMs), which can be attributed to the cost of ordering hydroxyl and carbonyl groups. Enthalpy–entropy compensation significantly lowered the ΔG of adsorption for all functionalised CNM ionic moieties, Fig. 2. a). Moreover, it made the adsorption ΔG of anionic CNT complexes exothermic, compared to the endothermic complexation of anionic PhACs on pristine CNTs , Fig. 2. a). Our findings are in accordance with a recent study which showed enthalpy–entropy compensation for small aromatic compounds adsorbed on a hydroxylated graphene surface [26]. At basic conditions with a pH value over 10, the hydroxyl groups of functionalised CNMs dissociate into $–O^-$ and become engaged in Coulombic ionic interactions. The reason for this is the endothermic reaction for the complexation of all PhACs, except those with a high pK_a which form very stable complexes (e.g. carbamazepine, atenolol and propranolol). Our results are in accordance with experimental observations that report rapid decreases of adsorption for ketoprofen, diclofenac, naproxen [48,53–55] and an increase in adsorption for atenolol and propranolol [15] in alkaline conditions (pH>9). Finally, functionalization minimises the impact of all non-covalent interactions other than hydrogen bonds and introduces Coulombic ionic interactions. It results in lower (CNTs) or roughly the same (graphene) adsorption ΔG comparing to its pristine counterpart.

3.4 The effect of background solution

3.4.1 pH

pH is an important factor which influences the adsorption behaviour of PhACs by changing the charge state of the molecule. Increased pH (from 2 to 10) will lead to deprotonation of the functional groups on PhACs and will also deprotonate the hydroxyl groups on functionalised CNM surfaces. Because the complex stability ladder based on the adsorption ΔG is anion≤ neutral<cation for both pristine and functionalised CNMs (Fig. 2. a)), an increase in pH will have a negative influence on adsorption. Deprotonation of the functional groups of pharmaceuticals due to an increase in pH will change favourable cation-π interactions to π-π interactions (for basic PhACs) and π-π interactions to unfavourable anion-π interactions (for acidic PhACs). For functionalised CNMs, a high enthalpic gain of the cationic hydrogen bonded complexes will be reduced by switching to neutral hydrogen bonded complexes. In addition, at high pH, Coulombic electrostatic repulsion will occur between the negative functionalised CNMs and negative PhACs. Identical observations on the decreased adsorption of PhACs in alkaline conditions has been reported in several experimental studies [18,48,53–56]. An exception to this trend is displayed by those PhACs which do not change their ionic form over a pH range from 2 to 10 (i.e. carbamazepine, caffeine and primidone,) and, consequently, ΔG for the adsorption on pristine CNMs is constant, in accordance with experimental observations [16,18]. Another exception is an increase in adsorption ΔG for the interaction of carbamazepine, atenolol and propranolol with negatively charged functionalised CNMs due to favourable Coulombic ionic interactions, as discussed in previous paragraphs.

3.4.2 Solvent polarity

Electrostatic interactions and nonclassical hydrophobic effect are expected to behave differently as solvent polarity changes. The interplay of these effects is best observed as solvent polarity changes, Fig. 6. Hydrophobic interactions cause favourable complexation of pristine CNMs in water. On the other hand, electrostatic interactions modulate the impact of the hydrophobic effect. Low electric permittivity of *n*-octanol enhanced favorable cation–π interactions and lowered complexation energy differences. In contrast, enhanced unfavorable anion–π interactions caused larger differences between anionic complexes in water and *n*-octanol. The effect of solvent polarity on adsorption ΔG is not so pronounced for functionalised CNMs (Figure X) due to two reasons. Firstly, the introduction of OH groups decreased CNM surface hydrophobicity, thus reducing the hydrophobic effect in polar solvents and lowering the energy difference. Secondly, hydrogen bonds were partly formed in solvent-free areas which reduced the impact of the solvent on the strength of the hydrogen bonds, making the contribution of hydrogen bond enthalpies similar in both solvents. At first, our results are in contrast with those of Wei et. al. (2019) who reported a ~25 kJ mol^{-1} weaker interaction of neutral chlorophenol-based hormones with graphene oxide in non-polar solvents. However, they used a CNM model system with only one hydroxylic group and we speculate that one hydroxylic moiety did not decrease the CNM surface hydrophobicity enough to significantly lower hydrophobic interactions.

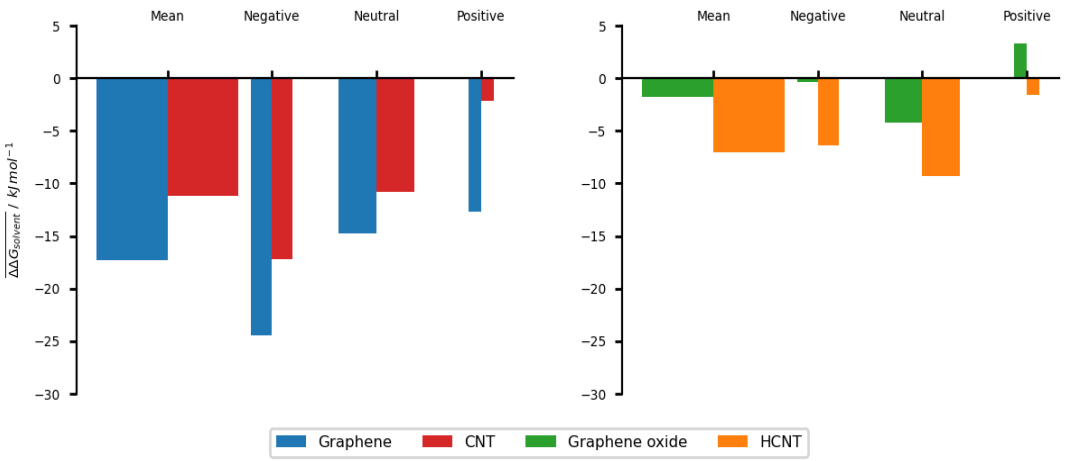

583

584 Fig. 6. Change of adsorption ΔG from water to *n*-octanol ($\Delta\Delta G_{solvent} = \Delta G_{water} - \Delta G_{n\text{-octanol}}$).
585 Overall mean $\Delta\Delta G_{solvent}$ is presented, as well as mean $\Delta\Delta G_{solvent}$ broken down by charge of a
586 complex.

587

588 ### 3.4.3 Temperature

589 Our calculations show negative ΔS values for all adsorption processes, suggesting that raising
590 the solution temperature will decrease ΔG and accordingly decrease adsorption (if present) of
591 the PhACs from the solution on the CNM. While our calculations agree with some
592 experimental observations about the negative effect of solution temperature on adsorption
593 behaviour [18,56], it disagrees with others [15,53].

594

595

596

597

3.5 Conditions for the efficient adsorption of PhACs on CNMs and subsequent regeneration of CNMs

ΔG of the adsorption of PhACs on CNMs is modulated by the properties of the PhACs, CNMs and the solution. With this knowledge, the adsorption process can be adjusted to favor or disfavor the removal of our ensemble of the 18 most common pharmaceuticals found in wastewaters [30]. Here we briefly assess different solution and CNM properties for achieving efficient adsorption. Details underpinning the reasoning can be found in the previous sections 3.4.1 and 3.4.2. Fig. 7. shows that graphene-based materials offer more favourable adsorption over CNTs, while pristine CNMs display slightly better adsorption at a low pH range. Pristine CNTs do not show spontaneous adsorption (except for positively charged PhACs) in the middle and high pH range. To summarise, functionalised CNMs display the strongest adsorption of PhACs in neutral conditions with an increase in pH causing a greater loss of adsorption strength than a decrease in pH. Pristine CNMs, on the other hand, display the strongest adsorption of PhACs in acidic conditions with a slower loss of adsorption strength as pH increases than was the case for functionalised CNMs.

Achieving peak performance of adsorption within the environmental (wastewaters) pH range is a huge benefit of functionalised CNMs considering their cost-effective application in wastewater treatment. Another benefit of functionalised CNMs is very low or no adsorption in the high pH range for most (except for a few very basic) pharmaceuticals. Effective desorption from pristine CNMs can be accomplished by reducing solvent polarity, preferably in the middle or low pH range. Effective desorption for both pristine and functionalised CNMs increases the reusability of an adsorbent, which in turn contributes to their cost effectiveness. In the end, it is important to have in mind that these results are based on model systems which may not perfectly reflect real life conditions.

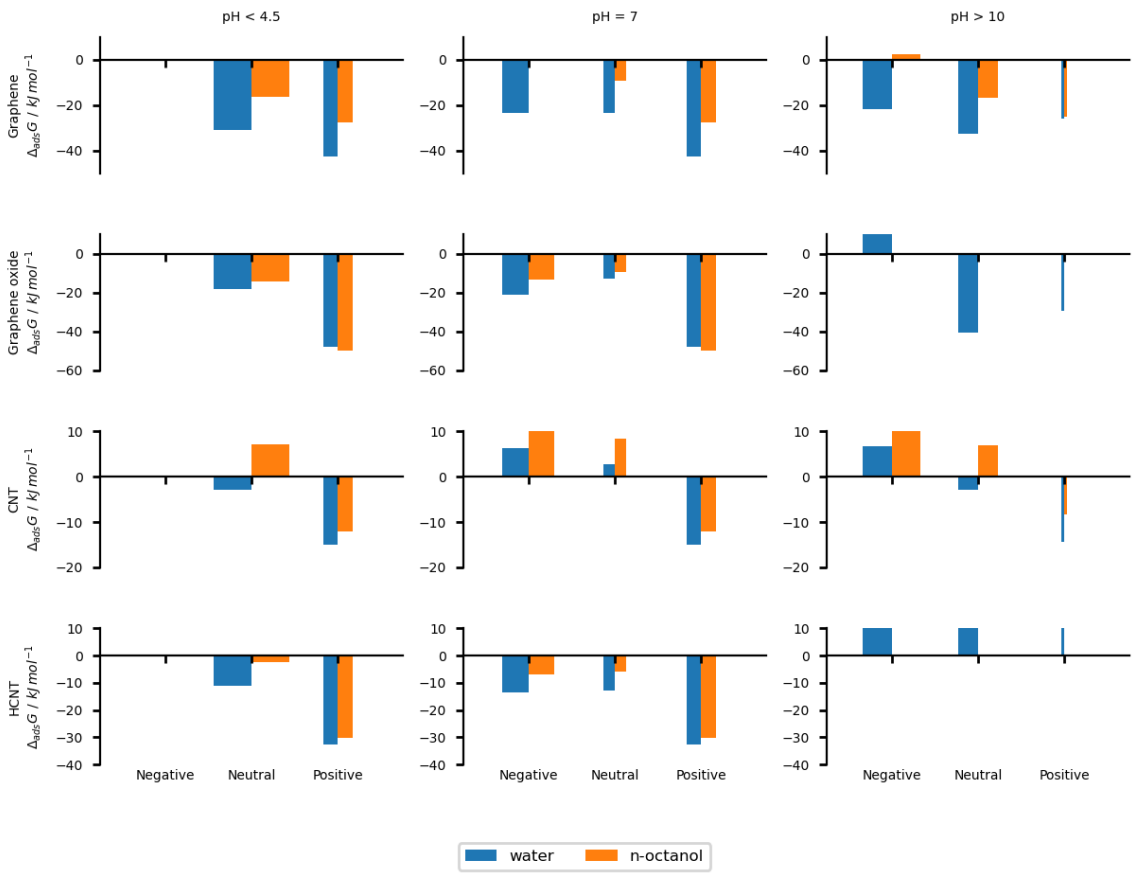

Fig. 7. Mean adsorption ΔG (at 283 K) for positive, neutral and negative complexes at different pH and solvent. Bar thickness is adjusted to the number of contributing complexes.

3.6 Understanding the ecotoxicity of PhACs – CNM complexes

The increased production and application of CNMs, as well as the weathering of CNMs will lead to their release into the environment. It is reasonable to believe that CNM debris will adsorb PhACs present in water. In addition, CNM debris will also adsorb dissolved organic matter, proteins and enzymes that stimulate cellular uptake of carbon nanoparticles by biota [57]. In a classical exposure scenario, aquatic organisms can ingest multi-stressor complexes

i.e. PhAC – CNM complex. Our data show that the transport of multi-stressor complexes through the gastrointestinal tract and blood of aquatic biota will not result in a significant change of adsorption energy for most of the PhACs studied, suggesting no release of these PhACs (Table S6, Supplementary material). This is due to the fact that water, the gastrointestinal tract and blood have a similar dielectric constant (Table S7, Supplementary material) and that the studied PhACs mostly will not change ionic form. Only diclofenac, ibuprofen, ketopofen, naproxen, gemfibrozil, fenofibric and clofibric acid may change their ionic form from negatively charged to neutral once they enter the abdomen and pH drops to the lowest physiological levels i.e. pH 3. A change to neutral ionic form will increase adsorption on pristine CNMs, in accordance with the observed trend of stability; neutral > anions, *vide supra*. However, most of the complexes with functionalised CNMs will exhibit a decrease of adsorption affinity, suggesting the potential latent release of these pharmaceuticals while in the abdomen at a pH below 4. Again, details explaining the observed behavior can be found in previous section 3.4.1.

While our data imply no release during transport through blood, the situation partly changes in the case of uptake across the epithelium and final cellular uptake. Intracellular pH is commonly around 7 and can vary from 4.5 to 8 depending on different organelles (Table S7, Supplementary material). Within that range, the ionic form of the studied pharmaceuticals and consequently their adsorption affinity will not change. However, the dielectric constant will range from 50 to 5 due to the presence of intracellular organelles and proteins, as well as a high content of lipid molecules (e.g. in cellular membranes and fat cells, Table S7, Supplementary material). A change in polarity will decrease the adsorption ΔG of all studied PhACs adsorbed on pristine CNMs and decrease adsorption ΔG of neutral and anionic PhACs adsorbed on functionalised CNMs (with exception of acetylsalicylic and fenofibric acid), suggesting the potential release of these pharmaceuticals in areas with low polarity, Fig 8. We

again need to stress that our discussion here is based on the change in adsorption ΔG of a model system with all its potential limitations.

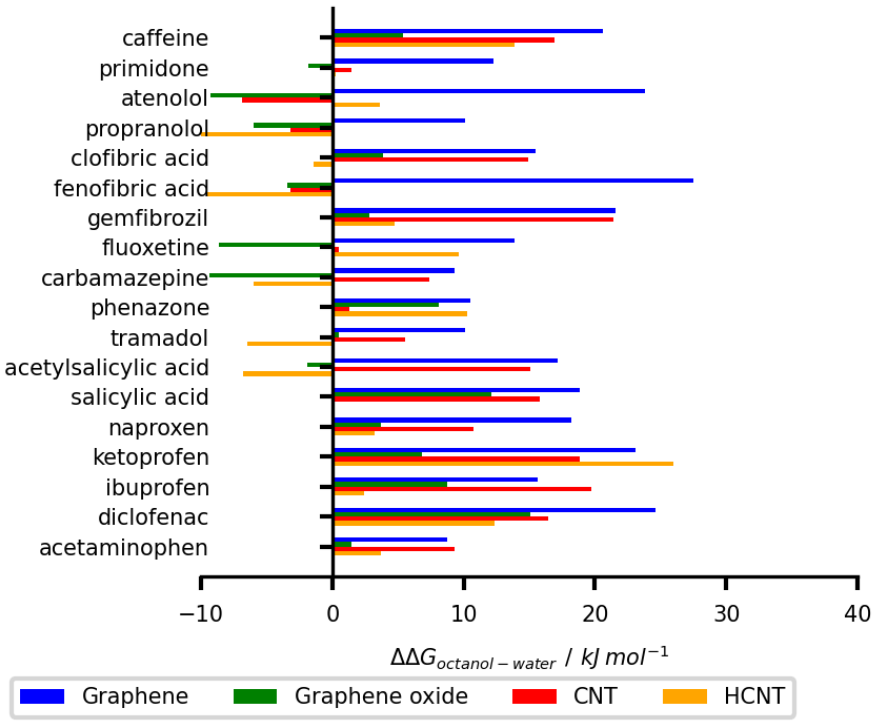

Fig. 8. Change of adsorption ΔG (at 283 K) due to transfer from high (water) to low (*n*-octanol) polar medium at pH 4.5-8. Positive value indicates higher $\Delta\Delta G_{\text{water-octanol}}$ i.e. desorption in low polar medium.

4. Conclusion

In this work, we computationally assessed the adsorption of 18 PhACs on four different CNMs in two different solvents. To the best of our knowledge, we presented the properties and adsorption thermodynamics of many PhAC-CNM complexes not yet studied experimentally.

Important findings of our work are summarised as follows:

Adsorption of PhACs on pristine CNMs, controlled by vdW dispersion forces, π interactions and hydrophobic interaction, exhibits the following stability ladder: cationic complexes > neutral complexes > anionic complexes. All complexes draw their stability from π–π and hydrophobic interactions; however, PhACs with larger π systems are more stable. The ratio between dispersion forces and ion-π interaction determines the stability of ionic complexes.

The functionalisation of CNMs minimises π interactions, but introduces hydrogen bonding and Coulombic ionic interactions. Delivered adsorption enthalpy gains are partly compensated by increased entropy. Strong hydrogen bonding has the largest impact on the stability of anionic complexes and changes the complex stability ladder to cation>neutral≈anion. Activation of Coulombic ionic interactions (at pH levels above 10) results in endothermic complexation of all PhACs except those with high pK_a.

Control of CNM curvature enables control of the contact surface (i.e. vdW and π interactions) and number of hydrogen bonds, primarily modulating the intensity of their contribution toward adsorption enthalpy.

The background solution controls many thermodynamic parameters through pH and solvent polarity. pH changes the charge distribution of both PhACs and hydroxylated CNMs, thus impacting electrostatic and hydrophobic interactions and, consequently, adsorption capacity.

690 Solvent polarity influences the hydrophobic effect, which is modulated by electrostatic
691 interactions.

692 The use of functionalised CNMs at environmental pH is the most effective method of removal
693 of a given set of PhACs. Washing with a basic water solution is the most cost-effective
694 method for the regeneration of the material. Problems, however, can arise with very basic
695 pharmaceuticals, which, under these conditions, still have low adsorption Gibbs free energy.

696 CNM debris can pose an environmental problem as they can adsorb and transport PhACs into
697 living organisms. Although PhAC-CNM complexes are stable, the potential release of PhACs
698 can happen in nonpolar mediums such as cellular membranes and fat cells.

699 We anticipate that the new data and insights into the mechanism of adsorption of PhACs on
700 CNMs under different conditions, along with the regeneration and ecotoxicity of CNMs
701 provided in this paper will contribute towards a design of CNMs for the effective removal of
702 PhACs from wastewaters, the evaluation of CNM toxicity, and towards the development of
703 predictive adsorption models.

704

705

Acknowledgements

The authors gratefully acknowledge the computing resources and support provided by The University Computing Centre (SRCE) in Zagreb. Proofreading by Katarina Cetinić (Ruđer Bošković Institute, Zagreb) is gratefully acknowledged. This work was supported by the Croatian Science Foundation project no. IP-2018-01-2298.

Supplementary material

Full geometries of the presented complexes are available upon request.

1. Supplementary material.docx

2. Table S2.xlsx

References:

[1] B. Petrie, R. Barden, B. Kasprzyk-Hordern, A review on emerging contaminants in wastewaters and the environment: Current knowledge, understudied areas and recommendations for future monitoring, Water Res. 72 (2015) 3–27. https://doi.org/10.1016/j.watres.2014.08.053.

[2] K.E. Arnold, A.R. Brown, G.T. Ankley, J.P. Sumpter, Medicating the environment: assessing risks of pharmaceuticals to wildlife and ecosystems, Philos. Trans. R. Soc. B Biol. Sci. 369 (2014) 20130569–20130569. https://doi.org/10.1098/rstb.2013.0569.

[3] A. Previšić, M. Rožman, J.R. Mor, V. Acuña, A. Serra-Compte, M. Petrović, S. Sabater, Aquatic macroinvertebrates under stress: Bioaccumulation of emerging contaminants and metabolomics implications, Sci. Total Environ. 704 (2019). https://doi.org/10.1016/j.scitotenv.2019.135333.

[4] A.C. Sophia, E.C. Lima, N. Allaudeen, S. Rajan, A.C. Sophia, E.C. Lima, N. Allaudeen, S. Rajan, Application of graphene based materials for adsorption of pharmaceutical traces from water and wastewater- a review, Desalin. Water Treat. 3994 (2016) 1–14. https://doi.org/10.1080/19443994.2016.1172989.

[5] K. Thakur, B. Kandasubramanian, Graphene and Graphene Oxide-Based Composites for Removal of Organic Pollutants : A Review, (2019). https://doi.org/10.1021/acs.jced.8b01057.

[6] B. Adhikari, M. Govindhan, A. Chen, Electrochimica Acta Sensitive Detection of Acetaminophen with Graphene-Based Electrochemical Sensor, Electrochim. Acta. 162 (2015) 198–204. https://doi.org/10.1016/j.electacta.2014.10.028.

[7] J. Wang, P. Zhang, B. Liang, Y. Liu, T. Xu, L. Wang, B. Cao, K. Pan, Graphene Oxide

as an Effective Barrier on a Porous Nanofibrous Membrane for Water Treatment, ACS Appl. Mater. Interfaces. 8 (2016) 6211–6218. https://doi.org/10.1021/acsami.5b12723.

[8] S. Yu, X. Wang, Y. Ai, X. Tan, T. Hayat, W. Hu, X. Wang, Experimental and theoretical studies on competitive adsorption of aromatic compounds on reduced graphene oxides, J. Mater. Chem. A. 4 (2016) 5654–5662. https://doi.org/10.1039/c6ta00890a.

[9] M. Zambianchi, M. Durso, A. Liscio, E. Treossi, C. Bettini, M.L. Capobianco, A. Aluigi, A. Kovtun, G. Ruani, F. Corticelli, M. Brucale, V. Palermo, L. Navacchia, M. Melucci, Graphene oxide doped polysulfone membrane adsorbers for the removal of organic contaminants from water Consiglio Nazionale delle Ricerche , Istituto per la Sintesi Organica e la Fotoreattività , Consiglio Nazionale delle Ricerche , Istituto per lo Studio , Chem. Eng. J. (2017). https://doi.org/10.1016/j.cej.2017.05.143.

[10] H. Zhao, X. Liu, Z. Cao, Y. Zhan, X. Shi, Y. Yang, J. Zhou, J. Xu, Adsorption behavior and mechanism of chloramphenicols, sulfonamides, and non-antibiotic pharmaceuticals on multi-walled carbon nanotubes, J. Hazard. Mater. 310 (2016) 235–245. https://doi.org/10.1016/j.jhazmat.2016.02.045.

[11] Y. Wang, Q. Yang, J. Dong, H. Huang, Science of the Total Environment Competitive adsorption of PPCP and humic substances by carbon nanotube membranes : Effects of coagulation and PPCP properties, Sci. Total Environ. 619–620 (2018) 352–359. https://doi.org/10.1016/j.scitotenv.2017.11.117.

[12] P. Taylor, J.L. Sotelo, A.R. Rodríguez, M.M. Mateos, S.D. Hernández, A. Torrellas, J.G. Rodríguez, Adsorption of pharmaceutical compounds and an endocrine disruptor from aqueous solutions by carbon materials, J. Environ. Sci. Heal. , Part B Pestic. Food Contam. Agric. Wastes. 47 (2012) 640–652.

https://doi.org/10.1080/03601234.2012.668462.

[13] H. Cho, H. Huang, K. Schwab, Effects of Solution Chemistry on the Adsorption of Ibuprofen and Triclosan onto Carbon Nanotubes, (2011) 12960–12967.

[14] S. Nam, C. Jung, H. Li, M. Yu, J.R. V Flora, L.K. Boateng, N. Her, K. Zoh, Y. Yoon, Adsorption characteristics of diclofenac and sulfamethoxazole to graphene oxide in aqueous solution, Chemosphere. 136 (2015) 20–26. https://doi.org/10.1016/j.chemosphere.2015.03.061.

[15] G.Z. Kyzas, A. Koltsakidou, S.G. Nanaki, D.N. Bikiaris, D.A. Lambropoulou, Science of the Total Environment Removal of beta-blockers from aqueous media by adsorption onto graphene oxide, Sci. Total Environ. 537 (2015) 411–420. https://doi.org/10.1016/j.scitotenv.2015.07.144.

[16] F. Liu, J. Zhao, S. Wang, P. Du, B. Xing, Effects of Solution Chemistry on Adsorption of Selected Pharmaceuticals and Personal Care Products (PPCPs) by Graphenes and Carbon Nanotubes, Environ. Sci. Technol. 48 (2014) 13197–13206.

[17] G. Moussavi, Z. Hossaini, M. Pourakbar, High-rate adsorption of acetaminophen from the contaminated water onto double-oxidized graphene oxide, Chem. Eng. J. 287 (2016) 665–673. https://doi.org/10.1016/j.cej.2015.11.025.

[18] L.A. Al-Khateeb, S. Almotiry, M. Abdel, Adsorption of pharmaceutical pollutants onto graphene nanoplatelets, Chem. Eng. J. 248 (2014) 191–199. https://doi.org/10.1016/j.cej.2014.03.023.

[19] R. Das, S.B. Abd Hamid, M.E. Ali, A.F. Ismail, M.S.M. Annuar, S. Ramakrishna, Multifunctional carbon nanotubes in water treatment: The present, past and future, Desalination. 354 (2014) 160–179. https://doi.org/10.1016/j.desal.2014.09.032.

[20] G. Ersan, O.G. Apul, F. Perreault, T. Karanfil, Adsorption of organic contaminants by graphene nanosheets: A review, Water Res. (2017). https://doi.org/10.1016/j.watres.2017.08.010.

[21] H. Tang, S. Zhang, T. Huang, F. Cui, B. Xing, pH-Dependent Adsorption of Aromatic Compounds on Graphene Oxide: An Experimental, Molecular Dynamics Simulation and Density Functional Theory Investigation, J. Hazard. Mater. 395 (2020) 122680. https://doi.org/10.1016/j.jhazmat.2020.122680.

[22] M. Zou, J. Zhang, J. Chen, X. Li, Simulating Adsorption of Organic Pollutants on Finite (8,0) Single- Walled Carbon Nanotubes in Water, Environ. Sci. Technol. 46 (2012) 8887–8894.

[23] J. Zhang, X. Lu, C. Shi, B. Yan, L. Gong, J. Chen, L. Xiang, H. Xu, Q. Liu, H. Zeng, Unraveling the molecular interaction mechanism between graphene oxide and aromatic organic compounds with implications on wastewater treatment, Chem. Eng. J. 358 (2019) 842–849. https://doi.org/10.1016/j.cej.2018.10.064.

[24] L. He, F. fei Liu, M. Zhao, Z. Qi, X. Sun, M.Z. Afzal, X. Sun, Y. Li, J. Hao, S. Wang, Electronic-property dependent interactions between tetracycline and graphene nanomaterials in aqueous solution, J. Environ. Sci. (China). 66 (2018) 286–294. https://doi.org/10.1016/j.jes.2017.04.030.

[25] Y. Ai, Y. Liu, Y. Huo, C. Zhao, L. Sun, B. Han, X. Cao, X. Wang, Insights into the adsorption mechanism and dynamic behavior of tetracycline antibiotics on reduced graphene oxide (RGO) and graphene oxide (GO) materials, Environ. Sci. Nano. 6 (2019) 3336–3348. https://doi.org/10.1039/c9en00866g.

[26] E.R.A. Singam, Y. Zhang, G. Magnin, I. Miranda-carvajal, L. Coates, R. Thakkar, H. Poblete, Thermodynamics of Adsorption on Graphenic Surfaces from Aqueous

812 Solution, J. Chem. Theory Comput. 15 (2019) 1302–1316.
813 https://doi.org/10.1021/acs.jctc.8b00830.

814 [27] Y. Wang, J. Chen, X. Wei, A.J. Hernandez Maldonado, Z. Chen, Unveiling Adsorption
815 Mechanisms of Organic Pollutants onto Carbon Nanomaterials by Density Functional
816 Theory Computations and Linear Free Energy Relationship Modeling, Environ. Sci.
817 Technol. 51 (2017) 11820–11828. https://doi.org/10.1021/acs.est.7b02707.

818 [28] D. Wei, C. Zhao, A. Khan, L. Sun, Y. Ji, Y. Ai, X. Wang, Sorption mechanism and
819 dynamic behavior of graphene oxide as an effective adsorbent for the removal of
820 chlorophenol based environmental- hormones : A DFT and MD simulation study,
821 Chem. Eng. J. 375 (2019) 121964. https://doi.org/10.1016/j.cej.2019.121964.

822 [29] I.M. Jauris, C.F. Matos, C. Saucier, E.C. Lima, A.J.G. Zarbin, S.B. Fagan, F.M.
823 Machado, I. Zanella, Adsorption of sodium diclofenac on graphene: A combined
824 experimental and theoretical study, Phys. Chem. Chem. Phys. 18 (2016) 1526–1536.
825 https://doi.org/10.1039/c5cp05940b.

826 [30] K.E. Murray, S.M. Thomas, A.A. Bodour, Prioritizing research for trace pollutants and
827 emerging contaminants in the freshwater environment, Environ. Pollut. 158 (2010)
828 3462–3471. https://doi.org/10.1016/j.envpol.2010.08.009.

829 [31] D. Daggag, J. Lazare, T. Dinadayalane, Conformation dependence of tyrosine binding
830 on the surface of graphene: Bent prefers over parallel orientation, Appl. Surf. Sci. 483
831 (2019) 178–186. https://doi.org/10.1016/j.apsusc.2019.03.181.

832 [32] N. Morimoto, T. Kubo, Y. Nishina, Tailoring the oxygen content of graphite and
833 reduced graphene oxide for specific applications, Sci. Rep. 6 (2016) 4–11.
834 https://doi.org/10.1038/srep21715.

[33] B. Konkena, S. Vasudevan, Understanding aqueous dispersibility of graphene oxide and reduced graphene oxide through p K a measurements, J. Phys. Chem. Lett. 3 (2012) 867–872. https://doi.org/10.1021/jz300236w.

[34] R. Sedlak, T. Janowski, M. Pitoňák, J. Rezáč, P. Pulay, P. Hobza, M. Pitoňák, J. Řezáč, Accuracy of Quantum Chemical Methods for Large Noncovalent Complexes, J. Chem. Theory Comput. 9 (2013) 3364–3374. https://doi.org/10.1021/ct400036b.

[35] A. V. Marenich, C.J. Cramer, D.G. Truhlar, Universal solvation model based on solute electron density and on a continuum model of the solvent defined by the bulk dielectric constant and atomic surface tensions, J. Phys. Chem. B. 113 (2009) 6378–6396. https://doi.org/10.1021/jp810292n.

[36] H.B. Schlegel, J.J.W. McDouall, Do You Have SCF Stability and Convergence Problems?, Comput. Adv. Org. Chem. Mol. Struct. React. (1991) 167. https://doi.org///doi.org/10.1007/978-94-011-3262-6_2.

[37] S.F. Boys, F. Bernardi, The calculation of small molecular interactions by the differences of separate total energies. Some procedures with reduced errors, Mol. Phys. 19 (1970) 553–566. https://doi.org/10.1080/00268977000101561.

[38] T. Lu, F. Chen, Multiwfn: A multifunctional wavefunction analyzer, J. Comput. Chem. 33 (2012) 580–592. https://doi.org/10.1002/jcc.22885.

[39] A. V. Iogansen, Direct proportionality of the hydrogen bonding energy and the intensification of the stretching ν (XH) vibration in infrared spectra, Spectrochim. Acta - Part A Mol. Biomol. Spectrosc. 55 (1999) 1585–1612. https://doi.org/10.1016/S1386-1425(98)00348-5.

[40] M.J. Frisch, G.W. Trucks, H.B. Schlegel, G.E. Scuseria, M. a. Robb, J.R. Cheeseman,

G. Scalmani, V. Barone, G. a. Petersson, H. Nakatsuji, X. Li, M. Caricato, a. V. Marenich, J. Bloino, B.G. Janesko, R. Gomperts, B. Mennucci, H.P. Hratchian, J. V. Ortiz, a. F. Izmaylov, J.L. Sonnenberg, Williams, F. Ding, F. Lipparini, F. Egidi, J. Goings, B. Peng, A. Petrone, T. Henderson, D. Ranasinghe, V.G. Zakrzewski, J. Gao, N. Rega, G. Zheng, W. Liang, M. Hada, M. Ehara, K. Toyota, R. Fukuda, J. Hasegawa, M. Ishida, T. Nakajima, Y. Honda, O. Kitao, H. Nakai, T. Vreven, K. Throssell, J. a. Montgomery Jr., J.E. Peralta, F. Ogliaro, M.J. Bearpark, J.J. Heyd, E.N. Brothers, K.N. Kudin, V.N. Staroverov, T. a. Keith, R. Kobayashi, J. Normand, K. Raghavachari, a. P. Rendell, J.C. Burant, S.S. Iyengar, J. Tomasi, M. Cossi, J.M. Millam, M. Klene, C. Adamo, R. Cammi, J.W. Ochterski, R.L. Martin, K. Morokuma, O. Farkas, J.B. Foresman, D.J. Fox, G16_C01, (2016) Gaussian 16, Revision C.01, Gaussian, Inc., Wallin.

[41] S. Gowtham, R.H. Scheicher, R. Pandey, S.P. Karna, R. Ahuja, First-principles study of physisorption of nucleic acid bases on small-diameter carbon nanotubes, Nanotechnology. 19 (2008) 125701 (6pp). https://doi.org/10.1088/0957-4484/19/12/125701.

[42] W. Wang, T. Sun, Y. Zhang, Y.B. Wang, Substituent effects in the ππ interaction between graphene and benzene: An indication for the noncovalent functionalization of graphene, Comput. Theor. Chem. 1046 (2014) 64–69. https://doi.org/10.1016/j.comptc.2014.07.017.

[43] D. Vijay, G.N. Sastry, The cooperativity of cation-π and π-π interactions, Chem. Phys. Lett. 485 (2010) 235–242. https://doi.org/10.1016/j.cplett.2009.12.012.

[44] A. Hosseini, S. Taylor, G. Accorsi, N. Armaroli, C.A. Reed, P.D.W. Boyd, Calix[4]arene-linked bisporphyrin hosts for fullerenes: Binding strength, solvation

effects, and porphyrin fullerene charge transfer bands, J. Am. Chem. Soc. 128 (2006) 15903–15913. https://doi.org/10.1021/ja066031x.

[45] M. Koné, B. Illien, J. Graton, C. Laurence, B3LYP and MP2 calculations of the enthalpies of hydrogen-bonded complexes of methanol with neutral bases and anions: Comparison with experimental data, J. Phys. Chem. A. 109 (2005) 11907–11913. https://doi.org/10.1021/jp054173s.

[46] C. Laurence, M. Berthelot, Observations on the strength of hydrogen bonding, Perspect. Drug Discov. Des. 18 (2000) 39–60. https://doi.org/10.1023/A:1008743229409.

[47] A.J.A. Aquino, D. Tunega, G. Haberhauer, M.H. Gerzabek, H. Lischka, Solvent effects on hydrogen bonds - A theoretical study, J. Phys. Chem. A. 106 (2002) 1862–1871. https://doi.org/10.1021/jp013677x.

[48] A.C.S. Guerra, M.B. de Andrade, T.R. Tonial dos Santos, R. Bergamasco, Adsorption of sodium diclofenac in aqueous medium using graphene oxide nanosheets, Environ. Technol. (United Kingdom). 0 (2019) 1–11. https://doi.org/10.1080/09593330.2019.1707882.

[49] P. Hobza, H.L. Selzle, E.W. Schlag, Potential energy surface for the benzene dimer. Results of ab initia CCSD(T) calculations show two nearly isoenergetic structures: T-shaped and parallel-displaced, J. Phys. Chem. 100 (1996) 18790–18794. https://doi.org/10.1021/jp961239y.

[50] E.M. Pérez, N. Martín, π-π Interactions in carbon nanostructures, Chem. Soc. Rev. 44 (2015) 6425–6433. https://doi.org/10.1039/c5cs00578g.

[51] K. Kanagaraj, M. Alagesan, Y. Inoue, C. Yang, Solvation Effects in Supramolecular

Chemistry, 2017. https://doi.org/10.1016/b978-0-12-409547-2.12481-3.

[52] S. Gotovac, H. Honda, Y. Hattori, K. Takahashi, H. Kanoh, K. Kaneko, Effect of nanoscale curvature of single-walled carbon nanotubes on adsorption of polycyclic aromatic hydrocarbons, Nano Lett. 7 (2007) 583–587. https://doi.org/10.1021/nl0622597.

[53] T. Van Tran, D.T.C. Nguyen, H.T.N. Le, D.V.N. Vo, S. Nanda, T.D. Nguyen, Optimization, equilibrium, adsorption behavior and role of surface functional groups on graphene oxide-based nanocomposite towards diclofenac drug, J. Environ. Sci. (China). 93 (2020) 137–150. https://doi.org/10.1016/j.jes.2020.02.007.

[54] Z. Ciğeroğlu, O.K. Özdemir, S. Şahin, A. Haşimoğlu, Naproxen Adsorption onto Graphene Oxide Nanopowders: Equilibrium, Kinetic, and Thermodynamic Studies, Water. Air. Soil Pollut. 231 (2020). https://doi.org/10.1007/s11270-020-04472-7.

[55] Y. Lu, Y. Li, Y. Gao, B.X. Ai, W. Gao, G. Peng, Facile preparation of 3D GO with caffeic acid for efficient adsorption of norfloxacin and ketoprofen, Water Sci. Technol. 81 (2020) 1461–1470. https://doi.org/10.2166/wst.2020.193.

[56] A.M.E. Khalil, F.A. Memon, T.A. Tabish, D. Salmon, S. Zhang, D. Butler, Nanostructured porous graphene for efficient removal of emerging contaminants (pharmaceuticals) from water, Chem. Eng. J. 398 (2020) 125440. https://doi.org/10.1016/j.cej.2020.125440.

[57] S.K. Smart, A.I. Cassady, G.Q. Lu, D.J. Martin, The biocompatibility of carbon nanotubes, 44 (2006) 1034–1047. https://doi.org/10.1016/j.carbon.2005.10.011.

[58] Lori A. Burns, Álvaro Vázquez- Mayagoitia, Bobby G. Sumpter, and C. David Sherrill, Density-functional approaches to noncovalent interactions: A comparison of dispersion

corrections (DFT-D), exchange-hole dipole moment (XDM) theory, and specialized functionals, J. Chem. Phys. 134 (2011) 084107. https://doi.org/10.1063/1.3545971

[59] M. K. Kesharwani, B. Brauer, J. M. L. Martin, Frequency and Zero-Point Vibrational Energy Scale Factors for Double-Hybrid Density Functionals (and Other Selected Methods): Can Anharmonic Force Fields Be Avoided?, J. Phys. Chem. A 119 (2015) 1701−1714. https://dx.doi.org/10.1021/jp508422u

[60] Chengyun Zhou, Zhuotong Zeng, Guangming Zeng, Danlian Huang, Rong Xiao, Min Cheng, Chen Zhang, Weiping Xiong, Cui Lai, Yang Yang, Wenjun Wang, Huan Yi, Bisheng Li, Visible-light-driven photocatalytic degradation of sulfamethazine by surface engineering of carbon nitride：Properties, degradation pathway and mechanisms, Journal of Hazardous Materials 380 (2019) 120815 https://doi.org/10.1016/j.jhazmat.2019.120815

[61] Xuerong Zhou, Zhuotong Zeng, Guangming Zeng, Cui Lai, Rong Xiao, Shiyu Liu, Danlian Huang, Lei Qin, Xigui Liu, Bisheng Li, Huan Yi, Yukui Fu, Ling Li, Zhihong Wang, Persulfate activation by swine bone char-derived hierarchical porous carbon: multiple mechanism system for organic pollutant degradation in aqueous media, Chemical Engineering Journal 383 (2019) 123091, https://doi.org/10.1016/j.cej.2019.123091